*Progress In Electromagnetics Research, Vol. 118, 287–301, 2011*

# A SLOW LIGHT FISHNET-LIKE ABSORBER IN THE MILLIMETER-WAVE RANGE

**M. Navarro-Cía[1,*], V. Torres[2], M. Beruete[2], and M. Sorolla[2]**

[1]Experimental Solid State Group, Department of Physics, Imperial College London, London SW72AZ, UK

[2]Millimeter and Terahertz Waves Laboratory, Universidad Pública de Navarra, Campus Arrosadía, Pamplona 31006, Spain

**Abstract**—A novel route to achieve a narrowband free-space electromagnetic absorber in any range of the spectrum based on stacked subwavelength hole arrays is proposed. The absorption is obtained by means of a slow light mode inside a fishnet-like engineered structure and exploiting the unavoidable misalignments and bucklings of the free-standing stack. An incoming pulse becomes permanently trapped in the structure due to the near zero group velocity which causes an enhancement of the radiation-structure interaction that leads to a huge increment of losses arising from the finite conductivity of the metal as well as arrangement tolerances. This approach is studied not only by simulation but also experimentally under normal incidence at millimeter wavelengths. Moreover, a basic grasp about the angular dependence of the structure is given by analyzing the 2D dispersion diagram. It shows that this scheme may also display high absorption under oblique incidence for *s*-polarization (or $TE$-polarization), whereas *p*-polarization ($TM$-polarization) would degrade its performance.

## 1. INTRODUCTION

The slow-light field has specially attracted a lot of interest since Hau et al. [1] reduced the group velocity of light to just 17 m/s in an ultracold gas of sodium atoms exhibiting electromagnetically induced transparency. Slow light has become a strong driving force for physicists and engineers since it has provided new exciting approaches

*Received 31 May 2011, Accepted 28 June 2011, Scheduled 5 July 2011*

* Corresponding author: Miguel Navarro-Cía (m.navarro@imperial.ac.uk).

in many areas such as nonlinear optics, quantum optics and all-optical information processing, lumping together both optical storage and switching, among others (see Refs. [2, 3] and references therein). Scientists in these fields race towards low loss systems, in order to improve the performance of the light-matter interaction.

The transmission through a subwavelength aperture was investigated by Bethe [4] and Bouwkamp [5] in the 1940s. They concluded that the transmission through a small hole on a planar infinite metallic screen under normal incidence was proportional to $(r/\lambda)^4$, where $r$ is the radius of the hole. Afterwards, Lewis et al. [6] used arrays of subwavelength holes for the development of the near-field scanning optical microscopy in the 1980s, showing that the array leads to a huge enhancement of the transmission. Nevertheless, it was Ebbesen and co-workers' paper [7] which gave the final boost to the research on the transmission through subwavelength holes, not only in the optical regime, but also in other regions of the spectrum. Initially, extraordinary optical transmission was ascribed to surface plasmons, but an alternative wider hypothesis was needed when this phenomenon was also replicated in millimeter waves, where surface plasmons make no sense [8–10]. This general explanation was reached under the framework of complex surface waves and diffraction [11].

In addition, a new topic called metamaterials has excited both physics and engineering communities since it seems to give access to exotic electromagnetic properties beyond the limits of natural media [12, 13]. A metamaterial is a composite medium consisting of subwavelength features that control the macroscopic electromagnetic response of the material. Some of this new accessible wide range of properties has allowed scientists to deal with trapped rainbow [3], perfect lens [14] and cloaking/invisibility [15] to name a few.

Moreover, a new growth in absorbing materials research and development has largely been driven by the progress in metamaterials. State-of-the-art of passive metamaterials for free-space absorber applications has evolved over the last years into four main strategies:

(i) Most of former ones resemble Salisbury single-screen by using a resistive sheet, a metamaterial/metasurface or even a simple frequency selective surface and a dielectric layer over a conductive ground plate in a resonator-like configuration, see Refs. [16–18].

(ii) On the other hand, some schemes have taken advantage of negative values of the real parts of the dielectric permittivity, $\epsilon$, and/or magnetic permeability, $\mu$, while neglecting losses [19]. The primary obstacle to achieve such a goal is the difficulty of producing the necessary resonance to get negative real parts of permittivity and/or permeability while imaginary ones are kept

low. This is the main reason why these approaches have been limited to microwaves, where losses can be reduced, although cannot vanish totally so as not to violate the Kramers-Krönig relations in causal systems [20].

(iii) Others have recently taken advantage of metamaterials losses [21] where the aforementioned relation in causal systems does not limit the performance of the scheme, giving this approach a brighter future as Ref. [22] confirms, especially in frequencies such as THz and optics, where metamaterial losses are a big concern.

(iv) Finally, the last trend is driven by optical transformation concepts [23, 24]. This approach holds huge potential. However, it requires precise fabrication procedures.

Recently, both phenomena, namely, extraordinary transmission (ET) and metamaterials, together with electromagnetic bandgap responses have been gathered together by means of stacking subwavelength hole arrays [25], see a picture in Figure 1. It was found that stacked hole arrays with a subwavelength stack period, support backward wave propagation, which leads to negative refraction in a prism configuration [26–28], whereas large longitudinal stack periodicities give rise to electromagnetic bandgap response with forward wave propagation for the first band. Remarkably and also relevant to this paper is that in the limit between both regimes, a zero group velocity mode, i.e., a slow light or frozen mode, appears [29]. Due to the periodicity (approximately $\lambda/2$) at which this phenomenon happens, it can be related to the excitation of a weakly coupled Fabry-Perot cavity resonance within the realm of electromagnetic bandgaps rather than metamaterials.

This work triggers discussion on the design, fabrication and experimental results of absorbers by means mainly of decelerating electromagnetic waves, i.e., slow light. This engineered frozen mode inside the structure brings about an increased metamaterial-field interaction which leads to losses rise, since the interaction between field and matter takes a longer time and the electric field intensity is enhanced as a result of the pulse compression. All these effects are further enhanced by the misalignments and bucklings of the free-standing stack. Notice that defects are indeed desired in this configuration. This scheme is totally contrary to the present aim of passive lossless slow-light systems research. Therefore, absorption effects described in this paper may be reminiscent of Refs. [21, 22], but the physics is substantially different since the loss enhancement is reached by a different mean. To the best of our knowledge, only slow light approaches based on magnetic-photonic crystals [30] and degenerate band-edge [31] have been used in free-space technology in

antenna field for gain enhancement and miniaturization [32, 33].

The work discussed in this paper could be a new guide for the design of similar absorbers in the THz and optical frequencies, since the four phenomena involved in the design are well-documented in these regimes (i.e., slow light, ET, electromagnetic bandgaps and Fabry-Perot resonances). However, further optimization is required to become competitive within the current proposals [16–18, 21–24, 34].

## 2. DESIGN AND SIMULATION RESULTS

As previously mentioned the key element to design a slow light medium with our strategy is the fishnet-like artificial structure, since by tuning adequately the longitudinal period, it enables us to engineer a frozen mode. The proposed ET structure, see Figure 1, consists of several subwavelength hole arrays perforated in aluminum plates whose unit cell parameters are: hole diameter $a = 2.5\,\text{mm}$, transversal lattice constants $d_x = d_y = d = 5\,\text{mm}$, metal thickness $w = 0.5\,\text{mm}$. For this particular set of parameters, ET emerges, for a single plate, around 57 GHz ($\lambda = 5.3\,\text{mm}$) although the individual hole starts to propagate at 70 GHz ($\lambda = 4.3\,\text{mm}$), that is, the cut-off frequency of the circular waveguide defined by the hole. Also, the longitudinal lattice constant, $d_z$, can be adjusted to achieve the required propagation mode with its associated field profile [25, 35]. In our case, we assign a fixed value

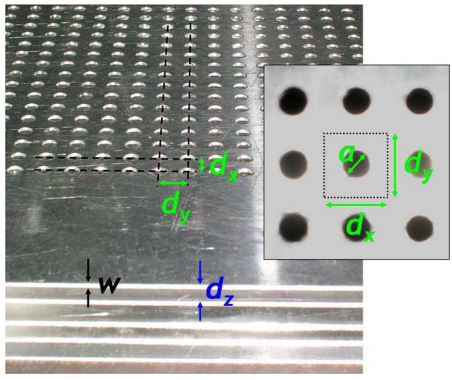


**Figure 1.** Photograph of the prototype and frontal picture of it highlighting the unit cell. Parameters: hole diameter $a = 2.5\,\text{mm}$, transversal lattice constants $d_x = d_y = d = 5\,\text{mm}$ and aluminium thickness $w = 0.5\,\text{mm}$. The longitudinal lattice constant, $d_z$, can be adjusted in order to obtain backward-wave, frozen regime or forward-wave propagation.

of $d_z = 2.5\,\text{mm}$ that corresponds to the frozen mode described in Refs. [29, 35]. Therefore, the modal pattern is susceptible to become irregular [36].

In order to realize how the proposed structure works, consider initially the 1D-dispersion diagram of the artificial medium ($z$-direction) under the assumption that we take just normal or close to normal incidence. This approximation allows us not to deal with the spatial/angular dispersion that all periodic composites have. This concern will be the subject later on in this paper.

The 1D-dispersion diagram of the infinite structure is calculated by using the eigenmode solver of the commercial software CST Microwave Studio$^{TM}$. To this end, a unit cell is taken and periodic boundary conditions are applied with a specific phase shift across the cell in the longitudinal dimension, i.e., the stack direction, whereas in the cross-sectional dimensions electric and magnetic walls for the $y$ and $x$ direction are employed respectively. The electromagnetic wave propagating in this artificial waveguide, thus, resembles the one of a TEM plane wave propagating along $z$-direction when the polarization is vertical (electric field along $y$) [29, 35].

The simulated dispersion diagrams, limited to the first propagating band and computed following the aforementioned method, are shown in Figure 2. The band corresponding to large longitudinal lattice constant (red trace) is shifted towards lower frequencies (longer wavelengths) and exhibits a positive slope, i.e., phase velocity parallel

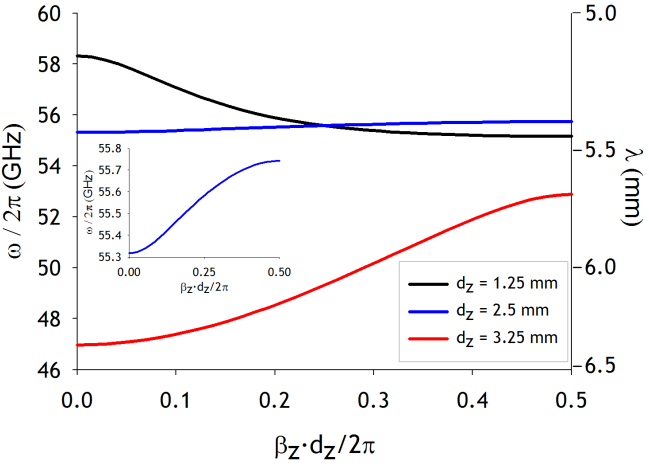


**Figure 2.** Simulated 1D dispersion diagrams for different longitudinal lattice constants.

to the group velocity, whereas the band related to close stacking (dark trace) shows a negative slope accounting for antiparallel phase and group velocities, i.e., backward wave propagation inside the stacked structure. Nevertheless, outstanding in this figure is that an intermediate stacking displays a near-zero slope, that is, a frozen mode (blue trace). It must be noted that the blue trace is not totally flat (see inset), but it may likely be achieved optimizing.

From the dispersion diagrams, the index of refraction is directly calculated through the relation (assuming lossless structures without loss of generality),

$$n_z = \frac{c}{v_p} = c\frac{\beta_z}{\omega} \tag{1}$$

which is directly proportional to speed of light in vacuum $c$, and inversely proportional to the slope of the line from the origin to the operating point on the dispersion diagram defined as it is in this work. The proportionality constant is the inverse of the longitudinal periodicity, $d_z$. Moreover, the group velocity is derived from the dispersion diagram as well,

$$v_{group,z} = \left(\frac{\partial\beta_z}{\partial\omega}\right)^{-1} = \left(\frac{\partial}{\partial\omega}\frac{\omega n_z}{c}\right)^{-1} = c\left(n_z + \omega\frac{\partial n_z}{\partial\omega}\right)^{-1} < c \tag{2}$$

which is obvious from the first equality that it is proportional to the slope of the dispersion diagram. Both the refractive index and the group velocity are plotted in Figures 3(a) and 3(b) respectively, for three different longitudinal lattice constants.

Let us now focus on Equation (2). It is clear that in order to achieve an ultraslow light mode either a high index of refraction or a

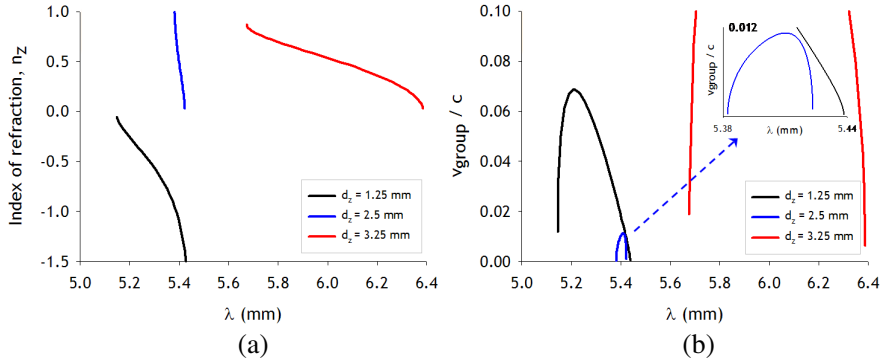


**Figure 3.** (a) Index of refraction. (b) Normalized group velocity for each propagation mode.

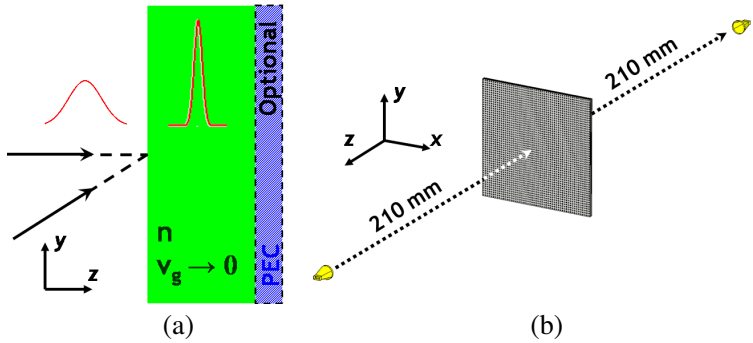


**Figure 4.** (a) Proposed scheme: a slab of stacked subwavelength hole arrays and optionally a conductive ground plate. (b) Sketch of the experimental setup.

rapid spectral variation of the index of refraction is mandatory. This is consistent with the numerical results depicted in Figure 3, i.e., with the fact that the frozen mode, $d_z = 2.5\,\text{mm}$, displays both the highest dispersion as well as the slowest group velocity within the three cases considered in this work.

The scenario corresponding to the approach proposed in this work is depicted on the left side of Figure 4. This scheme is simpler than those previously reported in the literature [16–19, 21–24] because of the reduction of the number of elements involved in it and the indifference toward defects-free structures. Due to the very low (ideally zero) group velocity related to this mode, the electromagnetic wave propagates very slowly inside the structure increasing the time that the radiation requires to pass through the structure as well as the electric field intensity due to the pulse compression (see Figure 4). This structure-field interaction eventually leads to an increment of the dissipated power. Furthermore, the impinging pulse suffers a compression, and its energy density is thereby increased, that is, the amplitude of the pulse rises, which amplifies the dissipation. Therefore, the incoming wave is absorbed by the engineered slab.

## 3. EXPERIMENTAL RESULTS AND DISCUSSION

A prototype of $54 \times 54$ holes has been fabricated in aluminum plates, see Figure 1, by drilling the hole array with the parameters detailed in previous section. By using our AB-Millimetre$^{TM}$ quasioptical vector network analyzer the transmission and reflection coefficients have been measured for a wavelength range of 4.7 mm–5.8 mm (51.7–63.8 GHz, V-

band). The experimental setup is schematically shown on the right side of Figure 4. It consists of an AB-Millimetre$^{TM}$, two corrugated horn antennas and the ET-based structure. The transmitter (continuous wave source) launches a vertically polarized Gaussian beam towards the sample, and the second antenna serves as a detector. This antenna is very sensitive to polarization and well matched to the Gaussian beam. The transmitting antenna also works as a receiver for the reflected power, using a directional coupler that steers the signal to the receiver. The transmission calibration of this setup configuration is done by simply removing the sample from the system and allowing the Gaussian beam to propagate. Conversely, the reflection calibration is done by removing the ET-based structure as well, but placing in this case a mirror in the sample holder. Notice that the radiation into higher order diffracted modes (emitting in other directions different from the normal) is negligible for this structure at the V-band [35].

The experimental result for the transmission and reflection coefficient of the $d_z = 2.5\,\text{mm}$ structure, that is, the slow light case, can be seen in Figure 5(a) for 3 different numbers of plates: 1 for comparison purposes, 4 and 10 stacked plates. A strong drop of the reflection is observed, while the transmission remains very low at around 5.5 mm, which is in agreement with the 1D dispersion diagram at about $\sim 98\%$. It is worth noting that ET-based structure shows

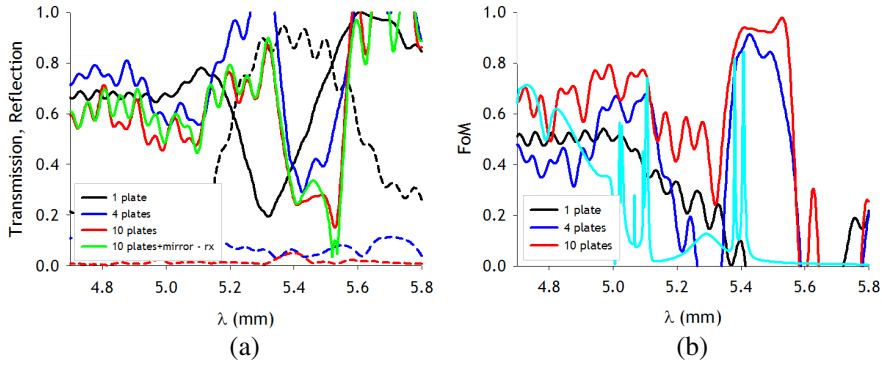


**Figure 5.** Experimental results: (a) shows transmission (dashed lines) and reflection (solid lines) of 1 plate (dark curves), 4 plates (blue curves) and 10 plates (red and green curves). The green curve corresponds to the system with a conductive plate at the back face of the artificial structure; (b) Illustrates the absorption of the system proposed for experimental: 1 (dark curve), 4 (blue curve) and 10 plates (red curve); simulation: 4 plates (cyan curve).

collimation when it is finite transversally [35, 37]. Therefore, it is in principle unexpected the low transmission recorded in this experiment. Besides, when a mirror is added at the rear part of 10 stacked perforated plates to totally annihilate transmission, reflection remains almost unaltered comparing to the case without mirror. In other words, the absorption has been greatly increased, as it is highlighted in Figure 5(b), where the figure of merit is plotted computing it as follows: FoM $= 1 - |S_{21}|^2 - |S_{11}|^2$. Particular attention must be paid to this FoM since is not a true measure for the absorption of the structure, because of the collimation effect pointed out earlier. The collimation effect is readily seen for the one-plate structure in Figure 5(b), where the FoM is below zero (i.e., 5.4–5.7 mm range). This result would be incoherent for this passive system, unless it provided a beaming effect. Notice that the fast oscillations exhibited by the measurements and the reflection value above unity account for the normal-incidence-unavoidable standing-waves of the system.

It is worth commenting that in addition to the aforementioned collimation, absorption is indeed difficult to measure as, in the inherently finite real setup, it requires the angular integration of both transmitted and reflected signals. However, it is more accessible through a numerical calculation. Therefore, we compute numerically the total absorption of a fishnet-like structure comprising 4 perforated plates and infinite transversally with the aid of the frequency solver of CST Microwave Studio$^{TM}$ and its unit cell boundary condition. In order to model unavoidable defects, a shift of 0.25 mm has been introduced in layers 2 and 4. The result is plotted in cyan in Figure 5 and it catches somehow the main features of the experimental data. Notice that around our experimental absorption band, the simulation predicts 2 narrow absorption peaks, which may have merged together to form the measured absorption band. Needless to say, disagreements are expected because of other ignored misalignments, different illumination (Gaussian beam in the experiment and plane-wave in the simulation) and finite size of the sample that may broaden the resonances and reduces the Q-factor of the resonances shown by the numerical data, etc.

So far, we have simplified the problem to 1D, by assuming paraxial geometry. However, another matter of concern is the performance of the slab under oblique incidence illumination. Therefore, we take a further step toward accounting for the spatial/angular dispersion of the fishnet-like structure by analyzing the 2D-dispersion diagram (see Figure 6) which was calculated similarly to the 1D case. The dispersion diagrams give us a qualitative understanding of the behavior of the finite/real structure. Once again, the direction of the average phase

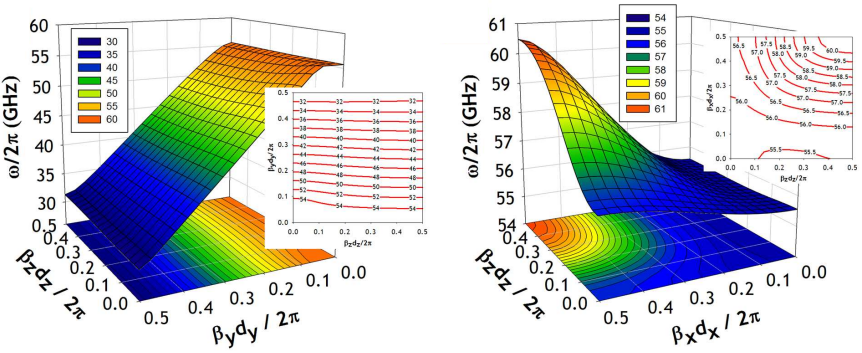


**Figure 6.** 2D-Dispersion diagram for (a) $p$-polarization and (b) $s$-polarization. To guide the eyes, equifrequency contour lines are highlighted on the right insets. It should be noted that each graph has its own colour scale.

velocity is parallel to $k$, whereas the direction of the average group velocity is given now by $\mathbf{grad}_k\ (\omega)$ [38], which is perpendicular to the $\omega$ contours and points in the direction of increasing $\omega$. A further revision of the oblique incidence for close stacking subwavelength hole arrays can be found in [39–42].

From Figure 6(a) one can directly infer that the performance of the system is strongly degraded for $p$-polarization oblique incidence, since the band moves rapidly towards lower frequencies, for increasing angle of incidence. However, despite this frequency shift, the frozen mode remains in the longitudinal dimension, $d_z$, which foresees a similar behavior of the system but in other frequencies. A different scenario occurs for $s$-polarized waves, see Figure 6(b). In this case, the band moves slowly towards higher frequencies, especially for small angles of incidence. Besides, in this range it remains a two-dimensional frozen mode, since $\mathbf{grad}_k\ (\omega) \to 0$. Therefore, it seems that the proposed system for new class of absorbers has a superior performance for $s$-polarization in terms angle of incidence dependence and for this polarization it can be used not only under normal incidence, but also under wide angles of incidence which we estimated to be around $\pm 11$ deg allowing a maximum frequency band shift of 0.3 GHz.

Finally, prominent in this approach is that even though each screen of the ET-based structure is practically metal, this fact does not affect the absorber performance. Total reflection expected in flat metals at millimeter wavelengths is dramatically cut down by the subwavelength-holes pattern despite the area of the hole per unit cell is only $\sim 0.2$.

## 4. CONCLUSIONS

The application of slow light to show the viability of constructing novel absorbers of the electromagnetic energy of a Gaussian beam by using extraordinary transmission fishnet-like structures is proposed and investigated experimentally in the millimeter wave range. The approach to slow light is founded on weakly coupled Fabry-Perot cavity resonance by interspacing free-standing subwavelength hole arrays approximately $\lambda_0/2$. The experimental results show good performance for the slow light scheme for normal incidence and numerical results suggest that *s*-polarized electromagnetic waves at the normal-incidence-design frequency might be even well absorbed for angles of incidence up to 11 deg. On the other hand, the strong angular dispersion associated to *p*-polarized waves prevents from good absorption properties under oblique incidence. As the extraordinary transmission was first reported in optics, we expect to be able to reproduce similar narrowband absorption behavior in both the visible as well as in THz frequencies because of the simplicity of this approach, although optimization is required to become competitive.

## ACKNOWLEDGMENT

The authors are grateful to Francisco Falcone and Nader Engheta for fruitful discussions. Work sponsored by the Spanish Government and E. U. FEDER funds under contracts Consolider Engineering Metamaterials CSD2008-00066 and TEC2008-06871-C02-01. M. N.-C. acknowledges support from Leverhulme Trust.

## REFERENCES

1. Hau, L. V., S. E. Harris, Z. Dutton, and C. H. Behroozi, "Light speed reduction to 17 metres per second in an ultracold atomic gas," *Nature*, Vol. 397, No. 6720, 594–598, 1999.
2. Krauss, T. F., "Why do we need slow light?," *Nature Photon.*, Vol. 2, No. 8, 448–450, 2008.
3. Tsakmakidis, K. L., A. D. Boardman, and O. Hess, "'Trapped rainbow' storage of light in metamaterials," *Nature*, Vol. 450, No. 7168, 397–401, 2007.
4. Bethe, H. A., "Theory of diffraction by small holes," *Phys. Rev.*, Vol. 66, Nos. 7–8, 163–182, 1944.
5. Bouwkamp, C. J., "On the diffraction of electromagnetic waves

by circular disks and apertures," *Philips Res. Rep.*, Vol. 5, No. 6, 401–422, 1950.

6. Lewis, A., M. Isaacson, A. Harrontunian, and A. Muray, "Development of a 500 Å spatial resolution light microscope: I. Light is efficiently transmitted through $\lambda/16$ diameter apertures," *Ultramicroscopy*, Vol. 13, No. 3, 227–231, 1984.
7. Ebbesen, T. W., H. J. Lezec, H. Ghaemi, T. Thio, and P. A. Wolf, "Extraordinary optical transmission through sub-wavelength hole arrays," *Nature*, Vol. 391, No. 6668, 667–669, 1998.
8. Beruete, M., M. Sorolla, I. Campillo, J. S. Dolado, L. Martín-Moreno, J. Bravo-Abad, and F. J. García-Vidal, "Enhanced millimeter-wave transmission through subwavelength hole arrays," *Opt. Lett.*, Vol. 29, No. 21, 2500–2502, 2004.
9. Beruete, M., M. Sorolla, I. Campillo, and J. S. Dolado, "Increase of the transmission in cut-off metallic hole arrays," *IEEE Microwave Wireless Compon. Lett.*, Vol. 15, No. 2, 116–118, 2005.
10. Beruete, M., M. Sorolla, I. Campillo, J. S. Dolado, L. Martín-Moreno, J. Bravo-Abad, and F. J. García-Vidal, "Enhanced millimeter wave transmission through quasioptical subwavelength perforated plates," *IEEE Trans. Antennas Propag.*, Vol. 53, No. 6, 1897–1903, 2005.
11. Lomakin, V. and E. Michielssen, "Transmission of transient plane waves through perfect electrically conducting plates perforated by periodic arrays of subwavelength holes," *IEEE Trans. Antennas Propag.*, Vol. 54, No. 3, 970–984, 2006.
12. Veselago, V. G., "The electrodynamics of substances with simultaneously negative values of $\epsilon$ and $\mu$," *Soviet Phys. Uspekhi*, Vol. 10, No. 4, 509–514, 1968.
13. Pendry, J. B., A. J. Holden, D. J. Robbins, and W. J. Stewart, "Magnetism from conductors and enhanced nonlinear phenomena," *IEEE Trans. Microwave Theory Tech.*, Vol. 47, No. 11, 2075–2084, 1999.
14. Pendry, J. B., "Negative refraction makes a perfect lens," *Phys. Rev. Lett.*, Vol. 85, No. 18, 3966–3969, 2000.
15. Schurig, D., J. J. Mock, B. J. Justice, S. A. Cummer, J. B. Pendry, A. F. Starr, and D. R. Smith, "Metamaterial electromagnetic cloak at microwave frequencies," *Science*, Vol. 314, No. 5801, 977–980, 2006.
16. Terracher, F. and G. Berginc, "A broadband dielectric microwave absorber with periodic metallization," *Journal of Electromagnetic Waves and Applications*, Vol. 13, No. 12, 1725–1741, 1999.

17. Engheta, N., "Thin absorbing screens using metamaterial surfaces," *IEEE Antennas Propag. Soc. (AP-S) Int. Symp. USNC/URSI Natl. Radio Sci. Mtg.*, Vol. 2, 392–395, San Antonio, 2002.
18. Bilotti, F., L. Nucci, and L. Vegni, "An SRR based microwave absorber," *Microwave Opt. Technol. Lett.*, Vol. 48, No. 11, 2171–2175, 2006.
19. Kisel, V. N. and A. N. Lagarkov, "Near-perfect absorption by a flat metamaterial plate," *Phys. Rev. E*, Vol. 76, No. 6, 065601-1–065601-4, 2007.
20. Jackson, J. D., *Classical Electrodynamics*, John Wiley & Sons, New York, 1998.
21. Landy, N. I., S. Sajuyigbe, J. J. Mock, D. R. Smith, and W. J. Padilla, "Perfect metamaterial absorber," *Phys. Rev. Lett.*, Vol. 100, No. 20, 207402-1–207402-4, 2008.
22. Tao, H., N. I. Landy, C. M. Bingham, X. Zhang, R. D. Averitt, and W. J. Padilla, "A metamaterial absorber for the terahertz regime: Design, fabrication and characterization," *Opt. Express*, Vol. 16, No. 10, 7181–7188, 2008.
23. Narimanov, E. E. and A. V. Kildishev, "Optical black hole: Broadband omnidirectional light absorber," *Appl. Phys. Lett.*, Vol. 95, No. 4, 041106-1–041106-4, 2009.
24. Cheng, Q., T. J. Cui, W. X. Jiang, and B. G. Cai, "An omnidirectional electromagnetic absorber made of metamaterials," *New J. Phys.*, Vol. 12, No. 6, 063006-1–063006-10, 2010.
25. Beruete, M., M. Sorolla, and I. Campillo, "Left-handed extraordinary optical transmission through a photonic crystal of subwavelength hole arrays," *Opt. Express*, Vol. 14, No. 12, 5445–5455, 2006.
26. Navarro-Cía, M., M. Beruete, M. Sorolla, and I. Campillo, "Negative refraction in a prism made of stacked subwavelength hole arrays," *Opt. Express*, Vol. 16, No. 2, 560–566, 2008.
27. Beruete, M., M. Navarro-Cía, F. Falcone, I. Campillo, and M. Sorolla, "Single negative birefringence in stacked spoof plasmon metasurfaces by prism experiment," *Opt. Lett.*, Vol. 35, No. 5, 643–645, 2010.
28. Navarro-Cía, M., M. Beruete, F. J. Falcone, M. Sorolla Ayza, and I. Campillo, "Polarization-tunable negative or positive refraction in self-complementariness-based extraordinary transmission prism," *Progress In Electromagnetics Research*, Vol. 103, 101–114, 2010.

29. Beruete, M., I. Campillo, M. Navarro-Cía, F. Falcone, and M. Sorolla Ayza, "Molding left- or right-handed metamaterials by stacked cutoff metallic hole arrays," *IEEE Trans. Antennas Propag.*, Vol. 55, No. 6, 1514–1521, 2007.
30. Figotin, A. and I. Vitebsky, "Nonreciprocal magnetic photonic crystals," *Phys. Rev. E*, Vol. 63, No. 6, 066609-1–066609-17, 2001.
31. Figotin, A. and I. Vitebsky, "Gigantic transmission band-edge resonance in periodic stacks of anisotropic layers," *Phys. Rev. E*, Vol. 72, No. 3, 036619-1–036619-12, 2005.
32. Yarga, S., K. Sertel, and J. L. Volakis, "Degenerate band edge crystals for directive antennas," *IEEE Trans. Antennas Propag.*, Vol. 56, No. 1, 119–126, 2008.
33. Mumcu, G., K. Sertel, and J. L. Volakis, "Miniature antennas and arrays embedded within magnetic photonic crystals," *IEEE Antennas Wirel. Propag. Lett.*, Vol. 5, No. 1, 168–171, 2006.
34. Atwater, H. A. and A. Polman, "Plasmonics for improved photovoltaic devices," *Nature Mat.*, Vol. 9, No. 3, 205–213, 2010.
35. Beruete, M., "Millimeter-wave extraordinary transmission: Connection to metamaterials and technological applications," Ph.D. Thesis, 2006.
36. Engelen, R. J. P., D. Mori, T. Baba, and L. Kuipers, "Two regimes of slow-light losses revealed by adiabatic reduction of group velocity," *Phys. Rev. Lett.*, Vol. 101, No. 10, 103901-1–103901-4, 2008.
37. Beruete, M., I. Campillo, J. E. Rodríguez-Seco, E. Perea, M. Navarro-Cía, I. J. Núñez-Manrique, and M. Sorolla, "Enhanced gain by double-periodic stacked subwavelength hole array," *IEEE Microwave Wireless Compon. Lett.*, Vol. 17, No. 12, 831–833, 2007.
38. Yeh, P., "Electromagnetic propagation in birefringent layered media," *J. Opt. Soc. Amer.*, Vol. 69, No. 5, 742–756, 1979.
39. Mary, A., S. G. Rodrigo, F. J. García-Vidal, and L. Martín-Moreno, "Theory of negative-refractive-index response of double-fishnet structures," *Phys. Rev. Lett.*, Vol. 101, No. 10, 103902-1–103902-4, 2008.
40. Beruete, M., M. Navarro-Cía, M. Sorolla, and I. Campillo, "Negative refraction through an extraordinary transmission left-handed metamaterial slab," *Phys. Rev. B*, Vol. 79, No. 19, 195107-1–195107-6, 2009.
41. Beruete, M., M. Navarro-Cía, and M. Sorolla, "Strong lateral displacement in polarization anisotropic extraordinary

transmission metamaterial," *New J. Phys.*, Vol. 12, No. 6, 063037-1–063037-15, 2010.

42. Beruete, M., M. Navarro-Cía, and M. Sorolla, "High numerical aperture and low-loss negative refraction based on the fishnet rich anisotropy," *Photon Nanostruct: Fundam Appl.*, 2011. doi: 10.1016/j.photonics.2011.04.009.